Closed-Loop Soft-Constrained Time-Optimal Control of Flexible Space Structures

M. Bikdash,* E. M. Cliff,† and A. H. Nayfeh‡
Virginia Polytechnic Institute and State University, Blacksburg, Virginia 24061

We propose numerically efficient solutions for the open- and closed-loop time-optimal soft-constrained control of a linear system representing a large flexible space structure. The open-loop solution is expressed in terms of the controllability Grammian matrix, for which we have obtained a closed-form expression for the undamped system. The qualitative dependence of the control on the initial state and the existence of many solutions satisfying the necessary conditions are shown. A nominal closed-loop control policy is subsequently formulated, but it is shown to be numerically expensive due to the nonuniqueness of extremal solutions. A continuation-based algorithm is proposed to alleviate the computational problem. Finally, the open- and closed-loop controls are shown to exhibit a saturation property reminiscent of the hard-constrained problem.

I. Introduction

THE problem of simultaneous slewing and vibration suppression of a large flexible space structure is a current research topic. The corresponding nonlinear partial-differential equations of motion are usually linearized, discretized in space, and truncated to a finite number of lightly damped modes. Several approaches to the control of large space structures have been investigated. The linear quadratic regulator and tracker problems[1] were successfully studied, and both open- and closed-loop controls were obtained. The simultaneous slewing and vibration suppression control problem of a rigid hub with flexible appendages was considered by Turner and Junkins[2] and Turner and Chun.[3] The latter included a control rate penalty in the cost function in order to smooth out the control functions and reduce control spillover to high-frequency modes. For the closed-loop case, a terminal state penalty was included. The drawback in a penalized terminal state is the numerical difficulty associated with a large terminal weighting matrix. Choosing a small terminal weighting matrix precludes accurate state regulation. An optimum choice of this matrix was proposed and systematically computed by Chun and Turner.[4] Closed-form expressions of the solutions of the resulting Riccati-like equations were obtained by Juang et al.[5] To avoid the problem associated with the terminal weighting matrix, they prescribed terminal constraints. A closed-form solution to a linear quadratic tracking problem with terminal state penalty was obtained by Turner et al.,[6] and a recursive formula was described by Juang et al.[7] Similar results for the regulator problem were obtained by Chun and Turner[8] and by Juang et al.[9]

A different approach to the solution of the linear quadratic regulator problem was considered by Breakwell.[10] The solution to the open-loop problem was obtained by evaluating the transition matrices corresponding to the two-point boundary value problem (TPBVP) obtained via Pontryagin's minimum principle. Breakwell stated that, for higher-order models, the transition matrices cannot be expressed analytically. He proposed a numerical scheme based on the eigenvector decomposition of the extended state-costate matrix. However, this approach was found to be numerically troublesome. Junkins[11] proposed using the diagonal Padé approximation to avoid these numerical difficulties. Breakwell[10] also showed how to deduce the closed-loop feedback formulation from the open-loop solution. However, this formulation runs into numerical difficulties near the origin because it requires the inversion of an almost-singular matrix. Hence, Breakwell proposed including a terminal state penalty instead of a terminal constraint. This alleviates the numerical problem somewhat but it does not eliminate it.

Time-optimal and mixed time-fuel-optimal controls of large flexible structures have recently received renewed attention. This problem is especially important in the case of three-axes rotation maneuvers of spacecraft. It is also important in the case of a flexible robot arm with a heavy payload. These two problems are not completely solved yet, and obtaining satisfactorily efficient feedback control strategies for higher-order systems is still an open research topic. In general, there are two approaches to the time-optimal problem. In the first approach, the control is hard constrained and is of the bang-bang type, which makes it suitable for nonthrottleable on-off thrusters. An approximate solution was attempted by Van der Velde and He[12] but its validity for a higher-order system has not been established. A different solution was proposed by Barbieri and Ozguner[13]; it is based on the symmetry property of the rest-to-rest maneuver of the undamped system. The solution is, hence, essentially an open-loop one. A numerical solution for a second-order system was proposed by Gnevko.[14] All of these methods cannot be generalized easily to higher-order systems. One approximate solution for the open-loop case that can be applied to a higher-order system was proposed by Thompson et al.[15]; it uses control shaping and approximates the bang-bang control by a smooth function. The nonlinear TPBVP is subsequently solved numerically. An exact solution proposed by Singh et al.[16] considered the TPBVP corresponding to the rest-to-rest maneuver for a linear undamped nongyroscopic system and reduced it to a system of nonlinear algebraic equations. In Refs. 15 and 16, homotopy methods had to be used in order to obtain reliable solutions. Meirovitch and Oz[17] proposed a solution using on-off controls in modal coordinates. This results in quantizable controls that could be implemented using clusters of on-off controllers. Meirovitch and Sharony[18] and Meirovitch and Quinn[19] proposed a control strategy based on a perturbation analysis. The rigid-body modes are controlled in a bang-bang, time-optimal fashion, and the vibrations of the flexible modes as well as the disturbances on the rigid modes are treated as a perturbation. The perturbing vibrations are suppressed using standard linear quadratic theory. Ben-Asher et al.[20] determined the switching

---

Received Oct. 26, 1990; revision received April 22, 1991; accepted for publication June 11, 1991.

*Graduate Student, Bradley Department of Electrical Engineering.
†Professor, Department of Aerospace and Ocean Engineering. Associate Fellow AIAA.
‡University Distinguished Professor, Department of Engineering Science and Mechanics. Associate Fellow AIAA.

times using a combination of a numerical nonlinear minimization scheme and a check of optimality. The approach is applicable to general high-order linear systems. The second approach to the minimum time/fuel problem is to penalize the control effort. This is the soft-constrained time-optimal problem. Ben-Asher and Cliff[21] obtained a numerical solution for this problem. Moreover, they applied a singular perturbation approach to decompose the high-order nonlinear TPBVP into a low-order nonlinear TPBVP and a high-order linear residual TPBVP.

In this paper, we consider the soft-constrained time-optimal control of a linear system. The solution of the open-loop problem must satisfy a nonlinear TPBVP derived from Pontryagin's principle. The solution is formalized in terms of the controllability Grammian, which is expressed in closed form for an arbitrary-order, undamped, nongyroscopic, linear system. Unfortunately, the extremal solution for the TPBVP is not unique, and there are many solutions corresponding to different values of the final time. These values are found by locating all of the roots of a scalar function of the form $H[t_f; x(0)] = 0$ computed in terms of the controllability Grammian. With this approach, the computational complexity does not change dramatically for a higher-order system but might be prohibitive for real-time applications. We study the open-loop solution and show a saturation and a bifurcation property. A closed-loop formulation is subsequently derived, and a continuation-type procedure is proposed for real-time, closed-loop, time-optimal control of high-order linear systems. Properties of this feedback control strategy are numerically illustrated.

II. Problem Formulation and Open-Loop Solution

A. Problem Formulation

The linear state-space model is

$$\dot{x}(t) = Ax(t) + bu(t) \tag{1}$$

where $x(t) \in \mathbb{R}^n$ and $u(t) \in \mathbb{R}$. Our study has been motivated by the analysis of a large solar panel whose dynamics is described in Sec. III.A. The open-loop, soft-constrained, time-optimal problem is to find a measurable function $u(t)$ that drives the state $x(0)$ to the target point $x(t_f) = 0$ while minimizing

$$J = h(t_f) + \frac{1}{2}\int_0^{t_f} \rho u^2(\tau)\,\mathrm{d}\tau, \qquad \rho > 0 \tag{2}$$

The cost function J is a weighted combination of the free final time and the control effort. We assume that $h(t_f)$ is a monotone increasing function and that the linear system is controllable. We define the variational Hamiltonian

$$\mathcal{H}(x,\lambda,u) = \tfrac{1}{2}\rho u^2 + \lambda^T(Ax + bu) \tag{3}$$

where $\lambda(t) \in \mathbb{R}^n$ is the costate vector. The optimal solution satisfies the combined state-Euler equations

$$\dot{x}(t) = Ax(t) + bu(t) \tag{4}$$

$$\dot{\lambda}(t) = -A^T\lambda(t) \tag{5}$$

$$u(t) = -\rho^{-1}b^T\lambda(t) \tag{6}$$

and the boundary conditions

$$x(0) \text{ given}, \qquad x(t_f) = 0 \tag{7}$$

$$H(t_f) \equiv \mathcal{H}\left[x(t_f), \lambda(t_f), u(t_f)\right] + h'(t_f) = 0 \tag{8}$$

Equations (4–8) constitute a nonlinear TPBVP. The differential equations are linear but the boundary condition $H(t_f) = 0$ is nonlinear in t_f. We note that, if t_f were given, the solution of the control problem could be obtained by solving the linear TPBVP given by Eqs. (4–7). The optimality of the assumed value of t_f can be checked using Eq. (8). The Euler-Lagrange equations can be written in the form

$$\begin{bmatrix} \dot{x}(t) \\ \dot{\lambda}(t) \end{bmatrix} = F\begin{bmatrix} x(t) \\ \lambda(t) \end{bmatrix}, \qquad F = \begin{bmatrix} A & -b\rho^{-1}b^T \\ 0 & -A^T \end{bmatrix} \tag{9}$$

where F is a Hamiltonian matrix.[22]

B. Solution in Terms of the Controllability Grammian

The solution of Eqs. (9) can be expressed in terms of the transition matrix $\Phi(t) = e^{Ft}$ as

$$\begin{bmatrix} x(t) \\ \lambda(t) \end{bmatrix} = \Phi(t)\begin{bmatrix} x(0) \\ \lambda(0) \end{bmatrix}$$

where

$$\Phi(t) = \begin{bmatrix} e^{At} & -e^{At}\rho^{-1}W(0,t) \\ 0 & e^{-A^Tt} \end{bmatrix} \tag{10}$$

where $W(0,t_f)$ is the controllability Grammian matrix given by

$$W(t_f) = \int_0^{t_f} v(\tau)v^T(\tau)\,\mathrm{d}\tau \tag{11}$$

and $v(t) = e^{-At}b$ is the time-reversed impulse response vector of the time-invariant system in Eq. (1). The controllability Grammian matrix arises in connection with the controllability of linear time-varying and time-invariant systems,[22,23] principal component analysis, and balancing techniques.[24] Efficient and reliable numerical algorithms for computing the controllability Grammian have been proposed recently (e.g., Refs. 24 and 25 and references therein), especially for the case of time-invariant systems with infinite horizon. The controllability Grammian matrix is symmetric (as is clear from its definition) and it is strictly positive definite for $t > 0$ if and only if the pair (A, b) is controllable.[22] In this case, the inverse of the controllability Grammian exists and it is symmetric and positive definite.

For $t = t_f$, Eq. (10) implies that $x(t_f) = 0 = e^{At_f}x(0) - e^{At_f}\rho^{-1}W(0,t_f)\lambda(0)$, or

$$W(0,t_f)\lambda(0) = \rho x(0) \tag{12}$$

It follows from Eqs. (12) and (5) that the costate vector is given by

$$\lambda(t) = e^{-A^Tt}\lambda(0) = \rho e^{-A^Tt}\left[W(0,t_f)\right]^{-1}x(0) \tag{13}$$

Moreover, it follows from Eqs. (6), (12), and (13) that the control function can be written as

$$u(t) = -\rho^{-1}v^T(t)\lambda(0) = -v^T(t)\left[W(0,t_f)\right]^{-1}x(0) \tag{14}$$

For $t = 0$, we have

$$u(0) = -b^T\left[W(0,t_f)\right]^{-1}x(0) = -y^T(t_f)x(0) \tag{15}$$

where $y(t_f)$ is given by

$$y(t_f) = \left[W(0,t_f)\right]^{-1}b \tag{16}$$

Furthermore, the cost function can be expressed in any of the following forms:

$$J = h(t_f) + \tfrac{1}{2}x^T(0)\lambda(0) = h(t_f) + \tfrac{1}{2}\rho x^T(0)\left[W(0,t_f)\right]^{-1}x(0) \tag{17}$$

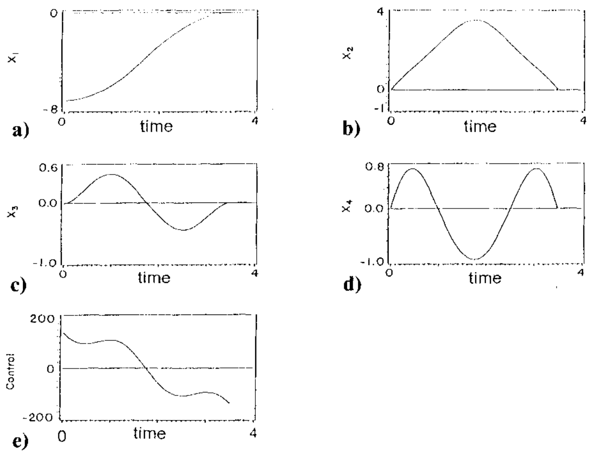

Fig. 1 Open-loop time-optimal control for one rigid-body mode and one flexible mode, $N = 1$, $n = 4$. A 7.25-deg slewing-angle rest-to-rest maneuver is conducted: a–d) system states; e) control function.

To determine the optimal final time, we substitute Eq. (6) into Eq. (8), evaluate the result at t_f, recall that $x(t_f) = 0$, and obtain

$$H(t_f) = h'(t_f) - \tfrac{1}{2}\rho^{-1}\left[b^T\lambda(t_f)\right]^2 = 0 \tag{18}$$

which, upon using Eqs. (12) and (13), can be written in the form

$$2\rho^{-1}h'(t_f) = \left[x^T(0)z(t_f)\right]^2 \tag{19}$$

where

$$z(t_f) = \left[W(0,t_f)\right]^{-1}v(t_f) \tag{20}$$

We note that Eqs. (18–20) imply that

$$b^T\lambda(t_f) = v^T(t_f)\lambda(0) = \rho x^T(0)z(t_f) = \sigma\sqrt{2\rho h'(t_f)} \tag{21}$$

where $\sigma = \pm 1$.

The roots of Eq. (19) specify all of the candidates for the minimum t_f. These roots can be found by solving Eq. (19) for t_f using any bracketing technique, such as the bisection method. If many roots $t_f^1, t_f^2, \ldots$ exist, the corresponding costs can be computed using Eq. (17). Direct comparison of the costs can then be used to find the globally minimizing value of t_f. Equations (12) and (14) can then be used to compute the open-loop optimal control.

One can show that the controllability Grammian satisfies the differential equation

$$\frac{\mathrm{d}W(0,t_f)}{\mathrm{d}t_f} = v(t_f)v^T(t_f) \tag{22}$$

We denote by $P(t_f)$ the inverse of the controllability Grammian, i.e., $P(t_f) = [W(0,t_f)]^{-1}$. It can be shown that $P(t_f)$ and $z(t_f)$ satisfy the differential equations

$$P'(t_f) = -z(t_f)z^T(t_f) \tag{23}$$

$$z'(t_f) = -\left[z(t_f)z^T(t_f) + P(t_f)A\right]v(t_f) \tag{24}$$

We note that Eq. (17) expresses the cost function as a function of the final time t_f, i.e., as $J(t_f)$. For an extremum of $J(t_f)$, it is necessary to have

$$\frac{\mathrm{d}J(t_f)}{\mathrm{d}t_f} = h'(t_f) - \frac{1}{2}\rho x^T(0)z(t_f)z^T(t_f)x(0) = 0$$

which is equivalent to Eq. (19). For a local minimum, it is sufficient to have

$$\frac{\mathrm{d}^2J(t_f)}{\mathrm{d}t_f^2} = h''(t_f) + z^T(t_f)v(t_f)\rho\left[x^T(0)z(t_f)\right]^2 + \left[x^T(0)z(t_f)\right]\lambda^T(0)Av(t_f) > 0 \tag{25}$$

Finally, we show an interesting control saturation property. Combining Eqs. (14) and (21), we obtain

$$u(t_f) = \pm\sqrt{2h'(t_f)/\rho} \tag{26}$$

which holds irrespective of the system dynamics defined by A and b and the initial state $x(0)$. In the case where $h(t_f) = t_f$, the control value at the final time depends exclusively on the weighting (design) parameter ρ. Equation (26) suggests the following definition of a significant and critical value of the control: $u_{cr} = \sqrt{2/\rho}$.

C. Numerical Considerations

First, we discuss several ways to numerically compute the controllability Grammian matrix. Two cases are to be distinguished. In the first case, the system matrix A does not possess any eigenvalue on the imaginary axis, and the controllability Grammian matrix can be expressed in the form[22]

$$W(0,\theta) = W_0 - e^{-A\theta}W_0e^{-A^T\theta} \tag{27}$$

where W_0 is a solution of the algebraic Lyapunov equation $AW_0 + W_0A^T = bb^T$, which is known to have a unique solution if no eigenvalue of the matrix A has zero real part. A second case is for the system in Sec. III.A, which has all of its eigenvalues on the imaginary axis. In this case, Eq. (27) cannot be used, but the controllability Grammian can be computed in closed form. A simple example is shown in Sec. III.A, and more general expressions can be found in Ref. 29.

In the following algorithms, one might need to compute $P(\theta)$, $W(0,\theta)$, $v(\theta)$, $z(\theta)$, and $e^{A\theta}$ accurately and efficiently. This can be done using any one of two extreme strategies:

1) If storage requirements are not prohibitive, one can evaluate off-line the quantities $e^{A\theta}$, $P(\theta)$, $z(\theta)$, and $v(\theta)$ at the points of the grid $\theta \in \{\theta_k = kT_\theta | \theta_L \le \theta_k \le \theta_H\}$. These values are then stored and subsequently used to compute P, z, and v at some arbitrary θ using interpolation.

2) If the computation time is not prohibitive, one can compute the controllability Grammian using Eq. (27) or Eq. (32), and then use Eqs. (20–24) to compute (and propagate) P, z, P', z', and v when needed.

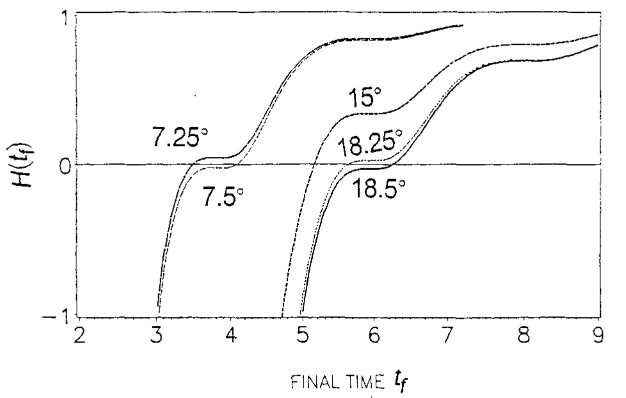

Fig. 2 Plot of $H(t_f)$ for different slewing angles. We note that an approximate point of tangency exists for the slewing angles of 7.35 and 18.35 deg, and we note the transversal character of the intersection of this curve with the line $H = 0$ for 15 deg.

III. Properties of the Open-Loop Control

A. Slewing of a Flexible Solar Panel

To illustrate the open-loop control, we consider the control of an aluminum beam that is 30 ft long and has a rectangular cross section with height 1 ft and thickness 0.25 in. This beam models a solar panel.[26] The system parameters are as follows.[27] The hub moment of inertia is 981 slug-ft^2, the beam rigidity is given by $EI = 3.49 \times 10^4$ lbf-ft^2, and the beam mass distribution is $m = 0.109$ slug/ft.

To obtain a finite-dimensional model, we use the assumed modes method[28] with a complete set of admissible functions given by $\phi_j(x) = (x/L)^j, j = 1,2,\ldots$. The natural frequency of the first flexible mode is given by $\omega_1 = 3.08$ rad/s. In this example, the natural frequencies are well spaced ($\omega_2 = 22.13$ rad/s). The control influence parameters are given by $g_0 = 0.0226$ and $g_1 = 0.0219$. For a general linear model with N retained flexible modes, we let x_1 represent the displacement of the rigid-body mode and x_2 its time derivative. Also, we let $x_3, x_5, \ldots, x_{2N+1}$ represent the displacements of the first, second, ..., Nth flexible modes, and $x_4, x_6, \ldots, x_{2N+2}$ represent their time derivatives. In this case, the state matrix A is given by

$$A = \begin{bmatrix} A_r & & 0 \\ & A_{f_1} & \\ & & \cdots \\ 0 & & A_{f_N} \end{bmatrix} \tag{28}$$

where A_r is a 2×2 matrix describing the rigid-body mode of the beam and A_{f_i} represents the ith flexible mode. They are given by

$$A_r = \begin{bmatrix} 0 & 1 \\ 0 & 0 \end{bmatrix}, \quad A_{f_i} = \begin{bmatrix} 0 & 1 \\ -\omega_i^2 & 0 \end{bmatrix} \quad \text{for } i = 1,2,\ldots,N \tag{29}$$

where ω_i is the natural frequency of the ith flexible mode and N is the number of retained flexible modes. The matrix b is given by

$$b^T = [0 \quad g_0 \quad 0 \quad g_1 \quad 0 \quad g_2, \ldots, 0 \quad g_N] \tag{30}$$

Hence, the time-reversed impulse response vector $v(t) = e^{-At}b$ is given by[29]

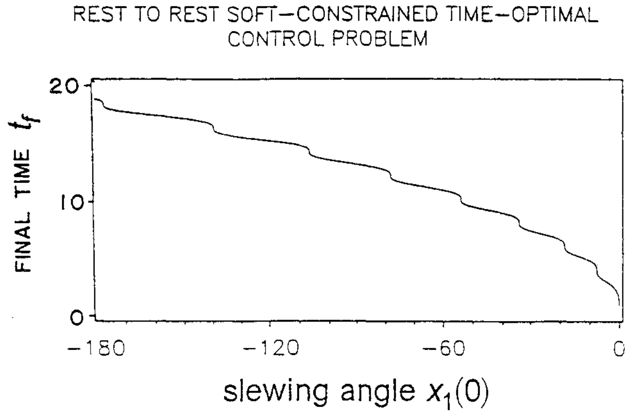

Fig. 3 Variation of the optimal final time with the slewing angle $x_1(0)$ in a rest-to-rest maneuver. We note the points of vertical tangencies at $x_1(0) \simeq -7.35, -18.35, -33.85, -53.65, -77.85, -106.65, -139.65$, and -177.15 deg.

B. Numerical Results

In the following simulations, we consider one flexible mode in addition to the rigid-body mode. Hence, $N = 1$, $n = 4$, and $\omega_1 = 3.08$. The weighting parameter is given by $\rho = 10^{-4}$, and $h(t_f) = t_f$.

Figures 1 show the rest-to-rest maneuver with a 7.25-deg slewing angle in the absence of parameter error and external disturbances. The origin is the target. We note the symmetry of the state trajectories and of the control function. Also, we note that Eq. (26) holds; that is, $|u(t_f)| = u_{cr} = \sqrt{2/10^{-4}} = 141.4$, which is also the value of $|u(0)|$ because of the symmetry of the rest-to-rest maneuvers.[27] Actually, for all of the subsequent rest-to-rest maneuvers, we observe that $|u(t)| \leq u_{cr} = 141.4$ for $0 \leq t < t_f$, and hence, by choosing ρ appropriately, one can guarantee that the control action stays within the physical limits of the actuators.

Figure 2 shows the function

$$H(t_f) = 1 - ½\rho \left[x^T(0) z(t_f)\right]^2$$

plotted vs t_f. The zeros of this function yield the values of t_f for which the cost function has a local extremum. This function has a unique zero for all rest-to-rest maneuvers.

$$v^T(t) = \left[-g_0 t, \quad g_0, \quad -\frac{g_1}{\omega_1}\sin\omega_1 t, \quad g_1 \cos\omega_1 t, \quad \ldots, \quad -\frac{g_N}{\omega_N}\sin\omega_N t, \quad g_N \cos\omega_N t \right] \tag{31}$$

The controllability Grammian can be expressed in closed form as $W(0,t) = V(t) - V(0)$, where $V(t)$ is defined by the indefinite integral

$$V(t) = \int^t v(\tau) v^T(\tau)\, d\tau$$

Closed-form expressions for an arbitrary number of modes can be found in Ref. 29. For one rigid-body mode and one flexible mode, $V(t)$ is given by

$$V(t) = \begin{bmatrix} \frac{1}{3} g_0^2 t^3 & \frac{-g_0^2 t^2}{2} & \frac{g_0 g_1}{\omega_1^2}\left(-t\cos\omega_1 t + \frac{\sin\omega_1 t}{\omega_1}\right) & \frac{-g_0 g_1}{\omega_1}\left(t \sin\omega_1 t + \frac{\cos\omega_1 t}{\omega_1}\right) \\ & g_0^2 t & \frac{g_0 g_1}{\omega_1^2}\cos\omega_1 t & \frac{g_0 g_1}{\omega_1}\sin\omega_1 t \\ \text{symmetric} & & \frac{g_1^2}{\omega_1^2}\left(\frac{t}{2} - \frac{\sin 2\omega_1 t}{4\omega_1}\right) & \frac{g_1^2}{2\omega_1^2}\cos^2\omega_1 t \\ & & & \frac{g_1^2}{2}\left(t + \frac{\sin 2\omega_1 t}{2\omega_1}\right) \end{bmatrix} \tag{32}$$

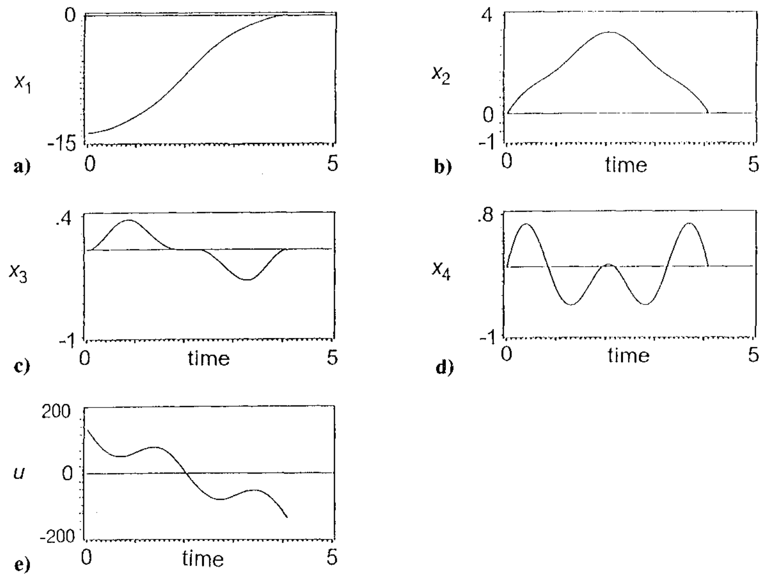

Fig. 4 Open-loop time-optimal control for one rigid-body mode and one flexible mode, $N = 1$, $n = 4$. A 7.5-deg slewing-angle rest-to-rest maneuver is conducted: a–d) system states; e) control function.

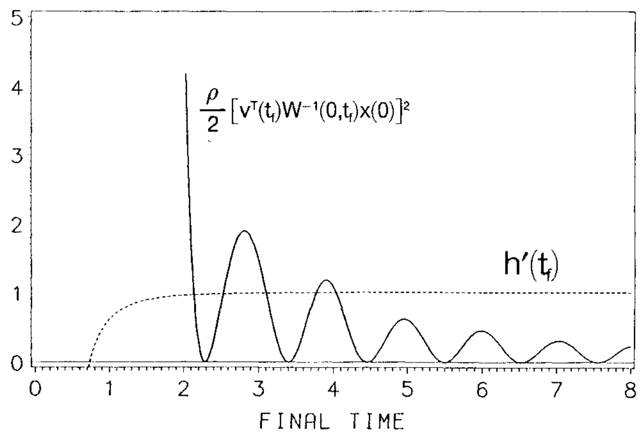

Fig. 5 Nonuniqueness of extremal solutions.

Figure 3 shows variation of the optimal final time with the slewing angle $x_1(0)$. The points of vertical tangencies represent bifurcation points, after which the flexible mode undergoes additional oscillations. This can be seen by comparing Figs. 1 and 4, representing maneuvers for slewing angles of 7.25 and 7.50 deg, respectively. These values are on opposite sides of the first vertical tangency. Through this bifurcation point, $x_1(t)$ and $x_2(t)$ undergo some minor differences, but $x_3(t)$ becomes tangential to the x_3 axis and $x_4(t)$ exhibits additional oscillations (three maxima in Fig. 4d as opposed to two maxima in Fig. 1d). Increasing the slewing angle from 7.5 to 18.25 deg (just before the second point of vertical tangency) does not change the number of oscillations of $x_4(t)$. Additional simulations have shown that this behavior is also true for the remaining points of vertical tangencies.

For maneuvers other than rest-to-rest maneuvers, there can be many values of t_f and, hence, of the initial costate, which satisfy the necessary conditions. These values of the final time can be found by locating all of the zeros of Eq. (19). For $h(t_f) = t_f + 0.2/t_f^2$, we show in Fig. 5 the two functions $h'(t_f)$ and $H_1(t_f) = \frac{1}{2}\rho[x^T(0)z(t_f)]^2$ whose intersections specify all of the values of t_f satisfying the necessary conditions for $x^T(0) \propto [0, 0, 0, 1]$. Clearly, there could be countably many such values. The globally minimizing value of t_f has to be determined by direct comparison of the corresponding costs. This nonuniqueness problem will considerably complicate the solution of the closed-loop control problem.

C. Modified Cost Function

It was found numerically that the condition number of $W(0,t_f)$ obtained from Eq. (32) satisfies the approximate relation $\log_{10}[\text{condition } W(0,t_f)] = 3.5 - 6.15 \log_{10}(t_f)$. Therefore, $W(0,t_f)$ becomes increasingly ill conditioned as $t_f \to 0$ and is not reliable for $t_f < 0.1$. Clearly, one should avoid assigning a very small value of t_f in order to avoid inverting a numerically ill-conditioned matrix. To insure numerical accuracy, we modify the cost function as to penalize on very small values of the final time; specifically, we define a new function

$$h(t_f) = t_f + \tau_1 t_f^{-\mu_1} + \tau_2 t_f^{-\mu_2} + \cdots = t_f + \sum_i \tau_i t_f^{-\mu_i} \tag{33}$$

where τ_i and μ_i are design parameters satisfying $\tau_i \geq 0$ and $\mu_i > 0$. We note that

$$h''(t_f) = \sum_i \mu_i(1+\mu_i)\tau_i t_f^{-\mu_i-2} > 0 \tag{34}$$

Therefore, $h'(t_f)$ is a monotone increasing function, and the equation $h'(t_f) = 0$ admits a unique root τ_f. It follows from Eq. (19) that the final time satisfies

$$t_f \geq \tau_f \tag{35}$$

A proper choice of τ_i and μ_i will specify a value for τ_f that guarantees a numerically well-conditioned controllability Grammian but that changes the effective value of the critical control u_{cr}. Additional design considerations can be used to specify τ_i and μ_i.

IV. Closed-Loop Solution

A. Nominal Feedback Control

An attractive feature of the above formulation is that it can be transformed into an optimal feedback control policy with relative ease, as was noted by Breakwell,[10] when the the final time t_f is finite and specified. Equation (15) can be interpreted as follows. For the initial state $x(0)$, the initial control that drives $x(0)$ to the origin optimally in a time t_f is given by Eq. (15). Since the time origin is arbitrary, we write Eqs. (12) and (15) as

$$\lambda(t) = \rho\left[W(0,\theta)\right]^{-1}x(t), \qquad u(t) = -y^T(\theta)x(t) \tag{36}$$

where θ is the optimal (minimum) time-to-go corresponding to $x(t)$. In the absence of any disturbances or modeling errors and for $h(t_f) = t_f$, one can argue[10] using Bellman's principle of optimality that $\theta = t_f - t$, $\forall\ 0 \le t \le t_f$, where t_f is the optimal final time necessary to take $x(0)$ to the origin. If the system is subjected to any disturbances or modeling errors, the optimal time-to-go θ ceases to be given by $\theta = t_f - t$, and it has to be updated to take into account the effect of disturbances. Strictly speaking, at an arbitrary time t, where the state is given by $x(t)$, θ is obtained by solving the nonlinear scalar algebraic equation [see Eq. (19)]

$$2\rho^{-1}h'(\theta) = \left[x^T(t)z(\theta)\right]^2 \tag{37}$$

for all its roots $\theta^1, \theta^2, \ldots, \theta^M$, where M is the number of roots; the roots depend on $x(t)$. Using Eq. (17), one can compute the corresponding costs $\{J(\theta^j)\}_{j=1}^M$ and, hence, determine the globally minimizing value of θ, denoted by θ^*. The control $u(t)$ can then be computed from Eqs. (36) using θ^*. If needed, the initial costate $\lambda^j(t)$ corresponding to θ^j can be found using Eqs. (36).

A true feedback policy requires the solution of Eq. (37) at every time t. Since no closed-form solution exists, we shall resort to a combination of sampled-data[30] and nominal or pseudofeedback solutions.[31] It consists of solving the open-loop problem at equally spaced sampling times $t_i = iT_s$, where T_s is the sampling period. The system state is then propagated according to

$$x(t_{i+1}) = A_D x(t_i) + b_D\left[u(t_i) + \mathrm{d}(t_i)\right]$$

where $\mathrm{d}(t_i)$ is a disturbance appearing as a torque at the hub, and $A_D = e^{AT_s}$ and

$$b_D = \int_0^{T_s} e^{A\tau} b \,\mathrm{d}\tau$$

characterize the discrete-time system model.

The pseudofeedback control policy is considerably complicated by the multiplicity of the roots of Eq. (37). As a result, the computations required for a full solution of Eq. (37) at each sampling instant are prohibitively large. In the following paragraphs, we develop a powerful continuation-type procedure to alleviate the computational problem.

We proceed in two steps. In Sec. IV.B, we use a perturbation analysis to obtain an approximation to the solution of the optimal control problem in the vicinity of a nominal extremal solution. By an extremal solution we mean a value of the time-to-go θ satisfying the necessary condition in Eq. (37), and the corresponding costate and cost. In Sec. IV.C, we describe the continuation algorithm that computes the globally minimizing solution.

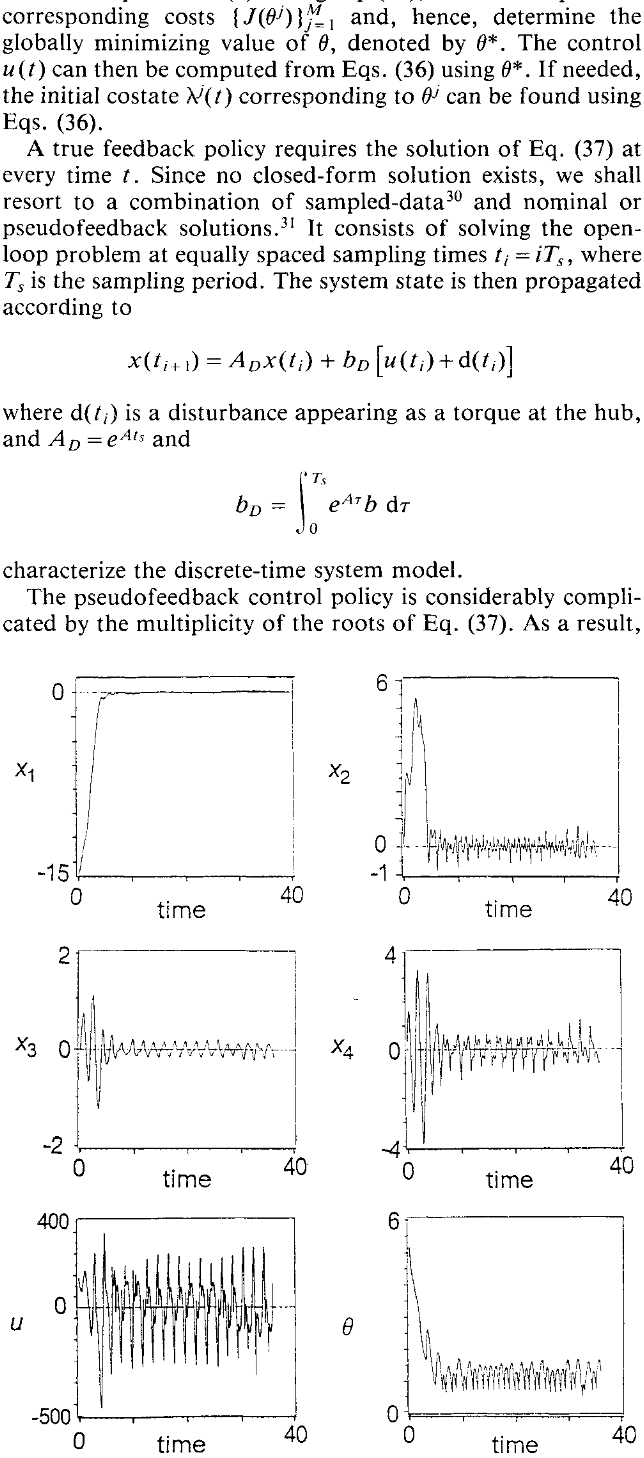

Fig. 6 Feedback controlled, 15-deg slewing angle, rest-to-rest maneuver under a sinusoidal disturbance $d(t) = 200\cos 3.2t$: initial condition $x_1(0) = -15$ deg; $h(t_f) = t_f + (0.2/t_f^2)$; $\rho = 10^{-4}$.

B. Perturbation Around a Nominal Solution

Let us consider a nominal (initial) state x, and let θ be one of the roots of Eq. (37). Let P, W, v, z, z', h, h', h'', λ, and J be the nominal quantities corresponding to the pair (x,θ). We assume a perturbation δx imposed on the state x, and we seek to determine the resulting perturbations $\delta\theta$, $\delta\lambda$, and δJ, corresponding to the nominal time-to-go, costate, and cost [see Eqs. (12), (17), and (19)], which satisfy the relations

$$\lambda(t) = \rho P(\theta)x(t), \qquad \left[x(t)^T z(\theta)\right]^2 = 2\rho^{-1}h'(\theta) \tag{38}$$

Perturbing the first equation and using Eqs. (20), (21), and (23), we obtain

$$\delta\lambda(t) = \rho P(\theta)\delta x(t) - \sqrt{2\rho h'(\theta)}\, z(\theta)\delta\theta \tag{39}$$

Perturbing the second equation and using Eqs. (21) and (24), we obtain

$$\delta\theta = -\frac{\rho\left[x^T(t)z(\theta)\right]\left[\delta x(t)^T z(\theta)\right]}{\rho\left[x^T(t)z(\theta)\right]\left[x^T(t)z'(\theta)\right] - h''(\theta)} \tag{40}$$

We note that if $h(\theta)$ is given by Eq. (33), then $h'(\theta) \to 1$ and $h''(\theta) \to 0$ as $\theta \to \infty$. In this case, Eqs. (39) and (40) become

$$\delta\lambda(t) \simeq \rho P(\theta)\delta x(t) - \sqrt{2\rho}\, z(\theta)\delta\theta$$

$$\delta\theta \simeq -\frac{\delta x^T z(\theta)}{x^T(t)z'(\theta)} \quad \text{as} \quad \theta \to \infty \tag{41}$$

Perturbing the equation $J = \theta + ½x^T(t)\lambda(t)$ [see Eq. (17)] and using Eqs. (39) and (40) yields

$$\delta J = \delta x^T(t)\lambda(t) \tag{42}$$

which makes sense since the costate describes the sensitivity of the cost function with respect to the state (see Ref. 1, p. 423).

C. Continuation Algorithm

The algorithm is based on two phases: reinitialization and propagation. In the reinitialization, one computes all of the roots θ of Eq. (37) in some interval $[\theta_{\min}, \theta_{\max}]$ accurately and without the use of prior information. In the propagation, one uses previously computed extremal solutions to estimate the current ones using the perturbation equations.

Reinitialization

The reinitialization is performed at $t = t_i = T_k$ for some i and k, where $T_{k+1} - T_k \gg T_s$. In the reinitialization routine, all of the roots of Eq. (37) in the interval $[\theta_{\min}, \theta_{\max}]$ are located by evaluating the function $H(t_f)$ at a grid of θ. The roots can be refined using bisection or golden-section search. The corresponding costs are then found using any of the forms in Eq. (17), and the globally minimizing value θ^* of θ is then determined.

Given all of the roots of Eq. (37) at some instant t_i, one can use Eq. (25) to determine whether a specific root actually leads to a local minimum, a local maximum, or an inflection point.

Clearly, we are only interested in local minima and only those should be propagated. We define the restricted set

$$\Theta(t_i) = \{\theta \mid \theta \text{ yields a local minimum of } J \text{ and } J(\theta)/J^* < r_1\} \tag{43}$$

where J^* is the global minimum of the cost function and $r_1 > 1$ is a parameter that is specified to eliminate values of θ that are unlikely to yield the globally minimizing θ^* before the next reinitialization.

Propagation

The propagation process is performed every sampling instant between two reinitializations; that is, at $t = t_i$ where $T_k < t_i < T_{k+1}$ for some k. This step consists of estimating $x(t_i)$, computing $\delta x_i = x(t_i) - x(t_{i-1})$, and using Eq. (40) to update $\Theta(t_{i-1})$ to form $\Theta(t_i)$ according the definition in Eq. (43). The globally minimizing value $\theta^*(t_i)$ is then determined by direct cost comparison. This globally minimizing value is then used to compute the control $u(t_i)$.

Of course, we would like to use the propagation routine as often as possible without accumulating substantial errors. Things can go wrong, however, due to estimation and round-off errors, points of vertical tangencies shown in Sec. III.B, jumps between competing local minima, and the creation of a new pair of one minimum and one maximum. To guard against these ills, we propose a strategy that switches to the reinitialization routine based on the following discrete-event interrupts. Specifically, we reinitialize if any of the following events occurs.

1) The time elapsed since the last reinitialization is greater than some value T_R.

2) $\delta\theta$ corresponding to any $\theta \in \Theta(t_i)$ is larger than some tolerance. This is to detect jumps due to a point of vertical tangency, where the correction $\delta\theta$ computed via Eq. (40) is expected to be inaccurate. In this case, we only need to accurately recompute the root undergoing the jump.

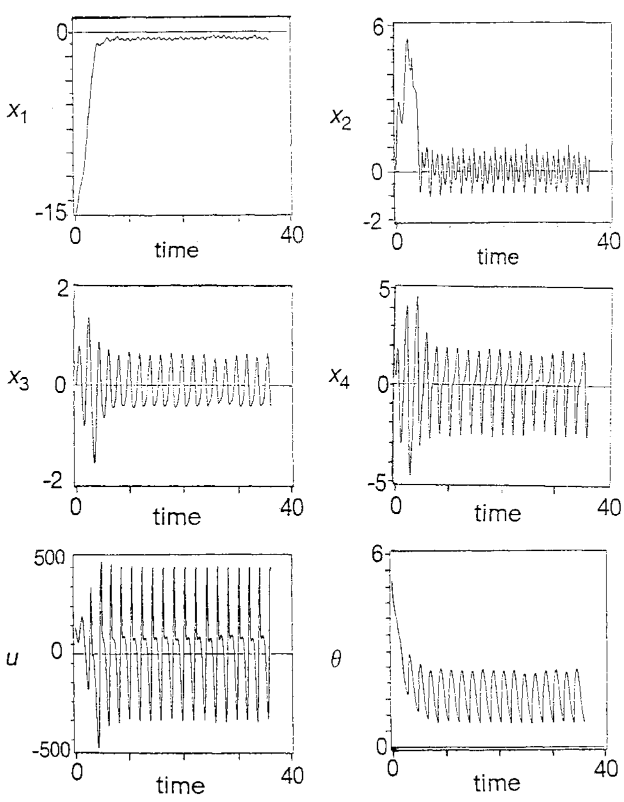

Fig. 7 Feedback controlled, 15-deg slewing angle, rest-to-rest maneuver under a sinusoidal disturbance of the form $d(t) = 250\cos 3.2t$: initial condition $x_1(0) = -15$ deg, $h(t_f) = t_f + (0.2/t_f^2)$, and $\rho = 10^{-4}$.

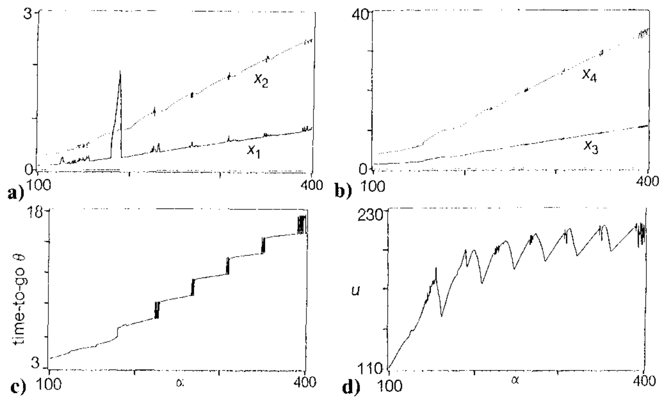

Fig. 8 Steady-state response of the time-optimal feedback controlled system vs the magnitude of the disturbance α: a) and b) steady-state magnitude of the states; c) peak value of the optimal time-to-go; d) peak value of the control function.

3) The estimated optimal time-to-go or the estimated optimal cost has changed unrealistically since the last reinitialization. This condition is detected if the optimal time to go at the current instant t_i is outside the range covered by $\Theta(T_k)$ at the previous reinitialization.

D. Numerical Simulations

We studied the response of the feedback-controlled undisturbed system for a rest-to-rest maneuver when $x_1(0) = -15$ deg, $h(\theta) = \theta + 0.02\theta^{-2}$, and $\rho = 10^{-4}$. We noted that the optimal time-to-go hits its floor τ_f specified by the parameters $\tau_1 = 0.2$ and $\mu_1 = 2$ in Eq. (33). We also studied the response of the time-optimal feedback-controlled system when subjected to a sinusoidal disturbance having the form $d(t) = \alpha\cos 3.2t$ and applied at the hub. The frequency of the disturbance is close to that of the natural frequency of the first flexible mode. For $\alpha = 100$, the feedback control quenches the disturbance satisfactorily. When the amplitude of the disturbance is increased up to $\alpha = 200$, the oscillations remain essentially small (Figs. 6.) The settling times for $\alpha = 10$ and 200 are near that necessary to conduct the open-loop maneuver for the undisturbed system. Increasing the forcing amplitude further to $\alpha = 250$ results in a sudden increase in the response amplitude, as shown in Figs. 7. This disturbance is too strong (compared with u_{cr}) for the feedback-control system to fully recover from the slewing maneuver, and the rigid-body mode oscillates around 1 deg instead of 0 deg as was the case in Figs. 6. This is another example of the nonlinear behavior of the system. When the forcing amplitude is increased far beyond the critical value $u_{cr} = \sqrt{2/\rho} = 141.4$, the performance of the control scheme deteriorates considerably, and the states oscillate violently (not shown). This case, however, occurs when the disturbance is much stronger than the available control action.

To illustrate the importance of the critical control value, we study the steady-state response of the feedback-controlled system as the forcing amplitude is varied. The result is shown in Figs. 8 for $\rho = 10^{-4}$ and $h(t_f) = t_f + (1/t_f) + (2/t_f^2)$. We note that the steady-state value of $x_1(t)$ has a peak at $\alpha = 190$, and the steady-state curves for all of the states change slope near this critical value of α. The peak value of the time-to-go (Fig. 8c) also changes character. Most significantly, we note that the peak value of the control saturates below the value $\alpha = 220$. These two values of the forcing amplitude (190 and 220) are close to $\sqrt{2}u_{cr}$. No theoretical justification of these observations is yet available. The sudden jump in the value of x_1 in Fig. 8a suggests the coexistence of many periodic steady-state solutions, each with its own domain of attraction in the state space. A more careful study is called for.

V. Conclusions

In summary, the continuation algorithm developed in this paper allows an efficient implementation of the soft-constrained time-optimal feedback control. For every root of the scalar nonlinear algebraic equation specifying the time-to-go, the algorithm requires twice as much storage as the linear quadratic regulator with fixed final time, and the amount of computations needed is the same order as the Kalman filter. The saturation property exhibited by the closed- and open-loop controls is reminiscent of the hard-constrained time-optimal control problem and it provides justification for a continued study of the soft-constrained time-optimal control as an alternative to the hard-constrained control, especially since the former is easier to obtain. What we really need to understand is the relation between the choice of $h(t_f)$, the effective critical-control value u_{cr}, and the saturation limits. Practical design procedures and a more exhaustive study of the properties of the developed algorithms are recommended.

References

[1]Kirk, D. E., *Optimal Control Theory,* Prentice-Hall, Englewood Cliffs, NJ, 1970.

[2]Turner, J. D., and Junkins, J. L., "Optimal Large-Angle Single-Axis Rotational Maneuvers of Flexible Aircraft," *Journal of Guidance, Control, and Dynamics,* Vol. 3, No. 6, 1980, pp. 578–585.

[3]Turner, J. D., and Chun, H. M., "Optimal Feedback Control of a Flexible Spacecraft During a Large-Angle Rotational Maneuver," *Proceedings of the AIAA Guidance and Control Conference,* AIAA Paper 82-1589, AIAA, New York, 1982.

[4]Chun, H. M., and Turner, J. D., "A Noniterative Algebraic Solution for Riccati Equations Satisfying Two-Point Boundary-Value Problems," *Journal of Optimization and its Applications,* Vol. 51, No. 4, 1986, pp. 355–362.

[5]Juang, J. N., Turner, J. D., and Chun, H. M., "Closed-Form Solutions for Feedback Control with Terminal Constraints," *Journal of Guidance, Control, and Dynamics,* Vol. 8, No. 1, 1985, pp. 39–43.

[6]Turner, J. D., Chun, H. M., and Juang, J. N., "Closed-Form Solutions for a Class of Optimal Quadratic Tracking Problems," *Journal of Optimization and its Applications,* Vol. 47, No. 4, 1985, pp. 465–481.

[7]Juang, J. N., Turner, J. D., and Chun, H. M., "Closed-Form Solutions for a Class of Optimal Quadratic Regulator Problems with Terminal Constraints," *Transactions of the ASME,* Vol. 108, March 1986, pp. 44–48.

[8]Chun, H. M., and Turner, J. D., "A Simple Algorithm for the Selection of Terminal Penalty Weighting Matrices," *Journal of Guidance, Control, and Dynamics,* Vol. 9, No. 4, 1986, pp. 503–505.

[9]Juang, J. N., Turner, J. D., and Chun, H. M., "Closed-Form Recursive Formula for an Optimal Tracker with Terminal Constraints," *Journal of Optimization and its Application,* Vol. 51, No. 2, 1986, pp. 307–321.

[10]Breakwell, J. A., "Optimal Feedback Slewing of Flexible Spacecraft," *Journal of Guidance, Control, and Dynamics,* Vol. 4, No. 5, 1981, pp. 472–479.

[11]Junkins, J. L., "Comment on Optimal Feedback Slewing of Flexible Spacecraft," *Journal of Guidance, Control, and Dynamics,* Vol. 5, No. 3, 1982, pp. 318,319.

[12]Van der Velde, W. E., and He, J., "Design of Structure Control Systems Using On-Off Thrusters," *Journal of Guidance, Control, and Dynamics,* Vol. 5, No. 1, 1983, pp. 53–60.

[13]Barbieri, E., and Ozguner, U., "Rest-to-Rest Slewing of Flexible Structures in Minimum Time," *Proceedings of the 27th IEEE Conference on Decision and Control,* Inst. of Electrical and Electronics Engineers, New York, 1988, pp. 1633–1638.

[14]Gnevko, S. V., "A Numerical Method for Solving the Linear Time-Optimal Control Problem," *International Journal of Control,* Vol. 44, No. 1, 1986, pp. 251–258.

[15]Thompson, R. C., Junkins, J. L., and Vadali, S. R., "Near-Minimum Time Open-Loop Slewing of Flexible Vehicles," *Journal of Guidance, Control, and Dynamics,* Vol. 12, No. 1, 1989, pp. 82–88.

[16]Singh, G., Kabamba, P. T., and McClamroch, N. H., "Planar, Time-Optimal, Rest-to-Rest Slewing Maneuvers of Flexible Spacecraft," *Journal of Guidance, Control, and Dynamics,* Vol. 12, No. 1, 1989, pp. 71–81.

[17]Meirovitch, L., and Oz, H., "Modal-Space Control of Large Flexible Spacecraft Possessing Ignorable Coordinates," *Journal of Guidance, Control, and Dynamics,* Vol. 3, No. 3, 1980, pp. 569–577.

[18]Meirovitch, L., and Sharony, Y., "Optimal Vibration Control of a Flexible Spacecraft During a Minimum-Time Maneuver," *Proceedings of the Sixth VPI/SU/AIAA Symposium on Dynamics and Control of Large Structures,* edited by L. Meirovitch, Virginia Polytechnic Inst. and State Univ., Blacksburg, VA, 1987.

[19]Meirovitch, L., and Quinn, R. D., "Equations of Motion for Maneuvering Spacecraft," *Journal of Guidance, Control, and Dynamics,* Vol. 10, No. 5, 1987, pp. 453–465.

[20]Ben-Asher, J., Burns, J. A., and Cliff, E. M., "Time-Optimal Slewing of Flexible Spacecraft," *Journal of Guidance, Control, and Dynamics* (to be published).

[21]Ben-Asher, J., and Cliff, E. M., "Soft-Constrained Time-Optimal Maneuvering of Flexible Spacecraft," *Proceedings of the 30th Israel Annual Conference on Aviation and Astronautics,* Israel, Feb. 1989, pp. 218–225.

[22]Brockett, R. W., *Finite Dimensional Linear Systems,* Wiley, New York, 1970.

[23]Kailath, T., *Linear Systems,* Prentice-Hall, Englewood Cliffs, NJ, 1980.

[24]Moore, B. C., "Principal Component Analysis in Linear Systems: Controllability, Observability and Model Reduction," *IEEE Transactions on Automatic Control,* Vol. 26, No. 1, 1981, pp. 17–30.

[25]Laub, A. J., Heath, M. T., Paige, C. C., and Ward, R. C., "Computation of System Balancing Transformations," *Proceedings of the IEEE 25th Conference on Decision and Control,* Inst. of Electrical and Electronics Engineers, New York, 1986, pp. 548–553.

[26]Turner, J. D., "Optimal Large Angle Spacecraft Rotational Maneuvers," Ph.D. Dissertation, Dept. of Engineering Science and Mechanics, Virginia Polytechnic Inst. and State Univ., Blacksburg, VA, May 1980.

[27]Ben-Asher, J., "Time-Optimal Slewing of Flexible Spacecraft," Ph.D. Dissertation, Dept. of Aerospace and Ocean Engineering, Virginia Polytechnic Inst. and State Univ., Blacksburg, VA, June 1988.

[28]Meirovitch, L., *Computational Methods in Structural Dynamics,* Sijthoff & Noordhoff, Rockville, MD, 1980.

[29]Bikdash, M., "Time-Optimal Control Techniques with Applications to Flexible Structures," Ph.D. Dissertation, Virginia Polytechnic Inst. and State Univ., Blacksburg, VA, 1991.

[30]Bryson, A. E., and Ho, Y. C., *Applied Optimal Control,* Hemisphere, New York, 1989.

[31]Cruz, J., *Feedback Systems,* McGraw Hill, New York, 1972.